Tropospheric Scintillation at *Ka*-Band Over a Hilly Tropical Region

Swastika Chakraborty, *Senior Member, IEEE*, Tapan Kumar Rana, and Saurabh Das, *Senior Member, IEEE*

***Abstract*—Satellite signal at the *Ka*-band is measured at a hilly, high rain fall region, Umiam, Shillong (25.6768° N, 91.9270 °E) for three years using GSAT 14 satellite. Scintillation has been extracted using a Butterworth filter of tenth order and 0.025 Hz cutoff frequency. Experimental results are then compared with the existing ITU-R scintillation model, Karasawa model, Van de Kamp model, and Ortgies-T model. Deviation of the above-mentioned models from measured data is then studied. The ITU-R model is found to be the best while Ortgies-T is found to be the worst performer over this region. New parameterization for the ITU-R scintillation model for the *Ka*-band is further proposed for this region based on one year of measured data and validated against other two years of data of 20.2 GHz. The results indicate the improved performance of the proposed model with a very high correlation value.**

***Index Terms*—*Ka*-band, orographic rain, rain attenuation, scintillation.**

I. Introduction

TROPOSPHERIC scintillation caused by turbulence driven fast fluctuation of refractive index within first Fresnel zone has a serious degrading effect for a low-fade-margin satellite communication link operating above 10 GHz. Raindrops absorb and scatter radio waves, which affect reliability of the received satellite signal badly, especially, in the GHz frequency range and known as rain attenuation. Rain and cloud also cause amplitude scintillation of the signal and degrade it further. Scintillation is generally quantified as log amplitude and log amplitude variance of the signal. The resulting field strength of the received signal is obtained by integrating over the antenna aperture.

The globally used International Telecommunication Union-Recommendation (ITU-R model[1]) for this purpose has a restriction of elevation angle, which becomes a serious issue in case of orographic rain over hilly locations. The theoretical model proposed by Tataraski [2] was based on the spatial model of atmospheric refractive index according to Kolmogorov spectrum only. On the other hand, the Karasawa [3] model predicts tropospheric scintillation based on the meteorological parameters over temperate region in the frequency range of 7–14 GHz and 4°–30° elevation angle. The Karasawa model was further modified for 40°–60° elevation angle for climate of Malaysia [4] considering measurement over Parit, Buntar, and then compared with the ITU-R model [1], the Otung model [5], and the Kamp model [6]. As water content of heavy cloud also has a very significant degrading effect in the form of scintillation, the Kamp model [6] incorporates the water content of heavy cloud as a parameter for the prediction of scintillation and has obtained very good agreement with the experimental results. Experimental measurements of tropospheric scintillation over Malaysia [7] have been carried out at 12 GHz frequency at 40° elevation angle and the results have been compared with all of the above-mentioned models. The Karasawa model and the Ortgies-T model have been found to have a good match with the measured values. The analysis of the worst month, seasonal and diurnal variation of enhancement and fade of tropospheric scintillation effect on propagation signal at 10.982 GHz over Malaysia was also carried out [8]. Suitable modification had been further proposed to the Karasawa model for predicting the signal amplitude due to tropospheric scintillation.

However, most of the studies reported so far were in the *Ku*-band and there is almost no report available on the *Ka*-band scintillation over tropical locations. Furthermore, the rain attenuation and scintillation characteristics due to orographic rain over hilly locations are almost nonexistent in the literature. Orographic rain influenced by hill topography may has a significant impact on rain and cloud characteristics and consequently on attenuation and tropospheric scintillation. Since there is an enhancement of rainfall intensity for most of the months of a year; temperature, pressure, and humidity also follow different patterns compared to plains. Therefore, these effects need to be studied separately in orographic rainfall regions for high-frequency applications.

In this letter, for the very first time, we are presenting the experimental study and validation of a few commonly used scintillation models over Shillong, a hilly tropical location in India.

II. Data Source

The satellite signal at 20.2 GHz has been received from GSAT-14 during the years 2017–2019 over hilly tropical location Umiam, Shillong (25.6768° N, 91.9270°E). Shillong receives

Manuscript received March 4, 2021; revised April 27, 2021; accepted May 2, 2021. Date of publication May 7, 2021; date of current version July 7, 2021. This work was supported by the DST-INSPIRE Faculty scheme and ISRO-RESPOND program. *(Corresponding author: Saurabh Das.)*

Swastika Chakraborty is with Sikkim Manipal Institute of Technology, Sikkim Manipal University, Gangtok 737102, India (e-mail: swastika1971@gmail.com).

Tapan Kumar Rana is with Institute of Engineering and Management, Calcutta 700091, India (e-mail: tkrana@rediffmail.com).

Saurabh Das is with Discipline of Astronomy, Astrophysics, and Space Engineering, Indian Institute of Technology, Indore 453552, India (e-mail: das.saurabh01@gmail.com).

Digital Object Identifier 10.1109/LAWP.2021.3078164

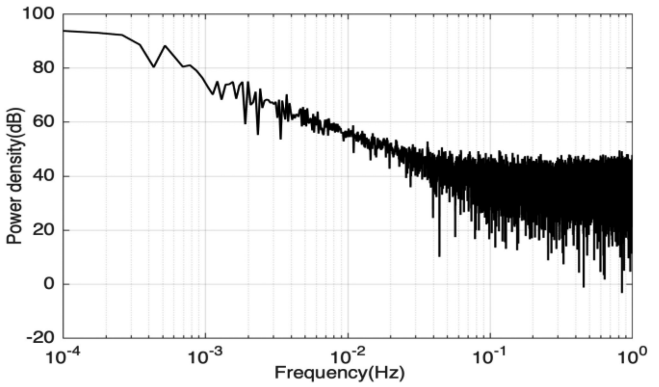

Fig. 1. Power spectral density of received signal in presence of rain of the day July 10, 2019, over Umiam, Shillong.

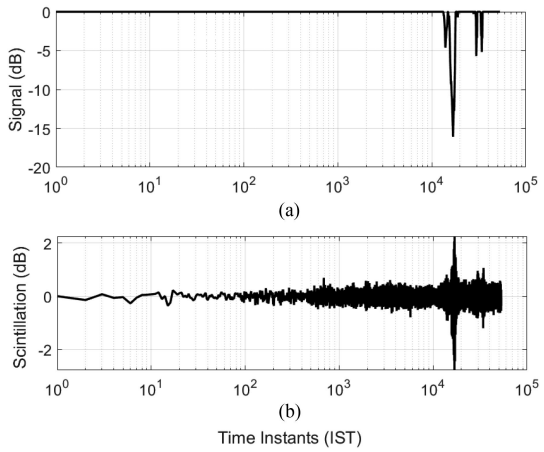

Fig. 2. (a) Attenuation of the day July 10, 2019, and (b) scintillation of the day July 10, 2019, over Umiam, Shillong.

annual average rainfall of 3385 mm with ∼130 rainy days per year. Average humidity of this place is 95% with a low cloud cover for more than 50% of the time of a year. The satellite signal is received at 58.53° elevation angle using a very small aperture terminal (VSAT) antenna in fixed polarization. The unmodulated beacon signal at 20.2 GHz from GSAT-14 satellite is received with 1 Hz temporal resolution. Signal power is measured by integrating across the whole band. Satellite signal is received as a voltage level initially. After required processing of signal, it is converted to decibel by taking the clear sky signal as reference level, which is received at low noise amplifier (LNA) input of the measurement system. The clear sky signal level is the combination of low-noise amplifier gain, antenna gain, loss in cable from spectrum analyzer to low noise amplifier, effective isotropic radiated power, and path loss from satellite to receiver.

Rainfall data are collected using the Thies Clima make laser precipitation monitor (LPM) with an integration time of 60 s. LPM basically senses the rain drops passing through a light beam by measuring the changes in the signal level and the time for drops to pass through the beam.

III. Methodology

Static power analysis of the received signal has been carried out to study the cutoff frequency between the low-frequency attenuation effect and the high-frequency scintillation effect. The power spectral density of the received signal, tracked on July 10, 2019, over Umiam, Shillong has been shown in Fig. 1 as an example.

To separate attenuation effect from the scintillation effect on received signal, it is then filtered through a Butterworth filter of the order 10 and threshold frequency of 0.025 Hz, as there is a visible difference in power density at that frequency. The Butterworth filter of the order 10 is chosen here comparing all other digital filters to match the stopband and to achieve the proper flatness in the output response. In Fig. 2, the received signal time series are plotted with the scintillation time series for July 10, 2019.

Constructive interference effect of the signal over antenna aperture is marked by positive scintillation or enhancement and destructive interference effect known as scintillation fade or negative scintillation. Enhancement of scintillation may lead to the system failure in case of multicarrier signal by increasing intermodulation noise for a satellite transponder. On the contrary, scintillation fade affects uplink power control system through length of time constant for that particular system. Both fade and enhancement of amplitude scintillation were studied and compared with the existing models. Scintillation fade depth is calculated from the standard deviation of the signal for the time period and propagation path. Standard deviation of the signal is derived from frequency, antenna averaging factor, elevation angle, and wet term of refractivity. Frequency and elevation angles are experimental parameters. The antenna averaging factor is calculated from the effective antenna diameter and the effective path length.

The wet term of refractivity is calculated from the relative humidity and the saturation water vapor pressure which, in turn, are calculated from the temperature. Therefore, fundamental input parameters are the temperature, the pressure, and the humidity of the place under consideration.

Furthermore, a model is developed for this location using one year of data and validated for other two years of data. These are described as follows.

IV. Results

A. Performance Comparison of Existing Scintillation Models

All the available recorded signal of 2017 to 2019 over Umiam, Shillong has been analyzed to have an understanding of the applicability of the available models for the prediction of scintillation. Fig. 3(a) shows the complementary cumulative distribution of worst month (June–September) scintillation amplitude of the years 2017–2019.

In Fig. 3(b), complementary cumulative distribution of experimentally measured scintillation amplitude is plotted along with ITU-R, Van-de-Kamp, Karasawa, Ortgies-N, and the Ortgies-T model predicted scintillation amplitude. Scintillation amplitude shows a higher value for this hilly tropical region as evident in

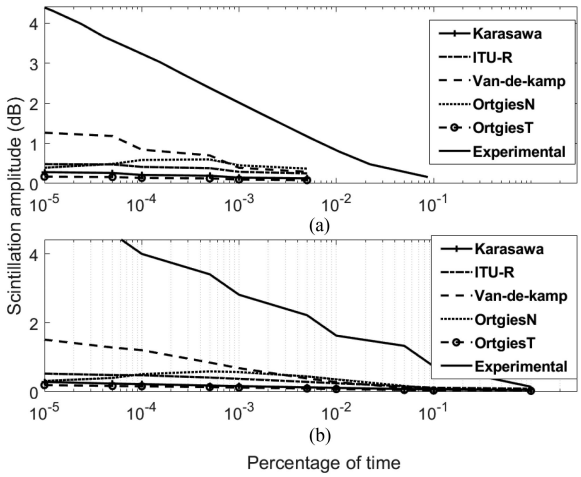

Fig. 3. (a) Complementary cumulative distribution of worst month scintillation amplitude of years 2017–2019. (b) Complementary cumulative distribution of scintillation amplitude of complete years 2017–2019.

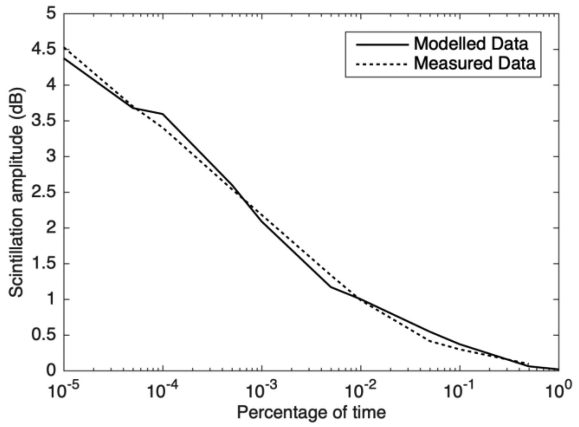

Fig. 4. Complementary cumulative distribution of scintillation amplitude of year 2018 (measured and fitted).

Fig. 3(b). It may be due to high annual average rainfall of this location. This may also be because of the fact that both the ITU-R and Karasawa model are developed on the data of temperate region and for the *Ku*-band frequency. The Karasawa model, specifically, is limited to the elevation angle from 4° to 30°. The Van de Kamp model and Ortgies model are also based on the data of temperate region.

B. Proposed Model of Tropospheric Scintillation for Shillong at Ka-band

The commonly used ITU-R model is chosen as the base model and modified to fit with the experimental data of this high rainfall hilly region. Here, turbulence layer height is taken as 1000 m along with the hilly regional meteorological parameters.

The standard deviation for radio propagation path and period is given by

$$\sigma = \sigma_{\mathrm{ref}} f^{1.182} \mathrm{g}(\mathrm{x}) / \sin\theta^{1.2}. \tag{1}$$

The time percent factor is given by

$$\begin{aligned} a(p) = & -0.061\left(\log_{10} p + m * \exp^{d*p} + c * \exp^{d*p}\right)^3 \\ & + 0.072\left(\log_{10} p + m * \exp^{b*p} + c * \exp^{d*p}\right)^2 \\ & - 1.71\log_{10}(p) + 3.0 \text{ for } 0.01 < p < 50 \end{aligned} \tag{2}$$

where $m = -0.9896$, $b = -0.55$, $c = 1.94$, $d = -117\ 2$ and $a(p)$ is the time percentage factor and σ is the standard deviation for radio propagation path.

For a percentage of time-fade depth of scintillation is

$$A_s(p) = a(p).\sigma. \tag{3}$$

V. New Model Performance Evaluation

In Fig. 4, proposed model calculated complementary cumulative exceedance of scintillation is plotted with the experimentally obtained complementary cumulative exceedance of scintillation for the year 2018.

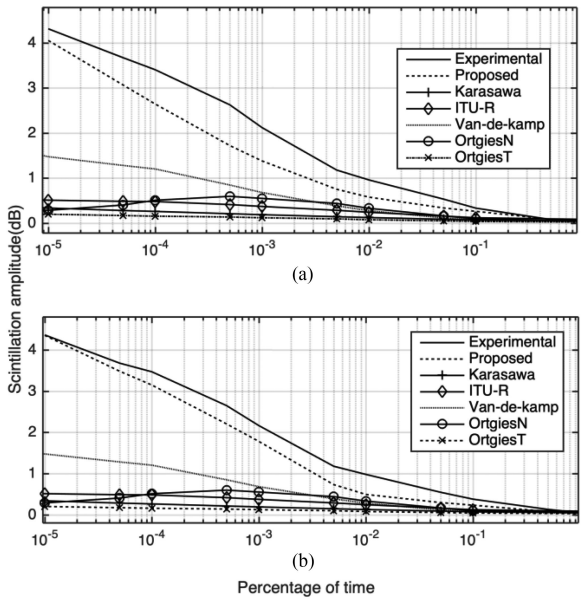

Fig. 5. (a) Complementary cumulative distribution of scintillation amplitude of year 2019. (b) Complementary cumulative distribution of scintillation amplitude of year 2017.

Agreement between the two curves shows that the proposed model can be used for finding the scintillation intensity of a high rainfall tropical region.

The newly developed model calculated cumulative distribution of scintillation for the year 2019 and 2017 are plotted with experimentally obtained values in Fig. 5(a) and (b), respectively.

Mean square error (MSE), root mean square error (RMSE), and correlation coefficient obtained from the existing models and new model with experimental data of 2017 and 2019 are given in Table I. Correlation coefficient value is 0.98 (maximum) for the proposed model indicating acceptable performance of the model. The maximum RMSE obtained between proposed model derived scintillation intensity and the experimentally obtained scintillation intensity are found to be 0.52 (maximum) as shown in Table I indicating a good performance of the proposed model.

TABLE I
MODEL PERFORMANCE

Name of the model	MSE	RMSE	Correlation Coefficient
ITU-R	6.2442	2.4988	0.971385
Karaswa	9.1111	3.01846	0.991277
Van de Kamp	4.288654	2.070907	0.991245
Ortgeis	4.559995	2.135415	0.972628
Proposed Model and 2017	0.10074	0.3174	0.983837
Proposed Model and 2019	0.27385	0.5233	0.9896

The primary reason for the unsatisfactory performance of existing models is due to the fact the rain induced scintillation is ignored in these models. The contribution of rain induced scintillation is significant in case of hill topography. Since the proposed model is based on the actual data, the rain contribution is accommodated in the proposed model. This may also be because of the fact that both the ITU-R and the Karasawa model are developed on the data of temperate region and for the *Ku*-band frequency.

VI. CONCLUSION

A new model at the *Ka*-band is proposed in this work for the prediction of scintillation intensity for this region based on the ITU-R model and experimental data of 2018. The performance of the proposed model is validated against two years of data (2017 and 2019). The RMSE and correlation coefficient between experimental and predicted data are found to be 0.52 and 0.98, respectively for the year 2019 and 0.31 and 0.98 for the year 2017, respectively, indicating the acceptable performance of the proposed model. However, more data from other locations are necessary for better evaluation of the proposed model.

ACKNOWLEDGMENT

The authors would like to thank the scientists of Space Applications Center, ISRO, for providing the experimental data.

REFERENCES

[1] *Propagation Data and Prediction Methods Required for the Design of Earth-Space Telecommunication Systems*, ITU R P.618, 2017.
[2] V. I. Tatarski,*Wave Propagation in a Turbulent Medium*. New York, NY, USA: McGraw-Hill, 1961.
[3] Y. Karasawa and J. F.A. M.Yamada, "A new prediction method for tropospheric scintillation on earth-space paths," *IEEE Trans. Antenna Propag.,* vol. AP-36, no. 11, pp. 1608–1614, Nov. 1988.
[4] C. C. Yee, J. .S. Mandeep, and M. .T. Islam, "Modification of Karasawa tropospheric scintillation model for Malaysia climate," *Indian J. Phys.*, vol. 89, pp. 841–845, 2013, doi: 10.1007/s12648-013-0305-5.
[5] I. E. Otung, "Prediction of tropospheric amplitude scintillation on a satellite link," *IEEE Trans. Antennas Propag.*, vol. 44, no. 12, pp. 1600–1608, Dec. 1996.
[6] M. M. J. L. van de Kamp, J. K. Tervonen, E. T. Salonen, and J. Pedro V. Poiares Baptista, "Improved models for long-term prediction of tropospheric scintillation on slant paths," *IEEE Trans. Antennas Propag.,* vol. 47, no. 2, pp. 249–260, Feb. 1999.
[7] J. S. Mandeep, "Extracting of tropospheric scintillation propagation data from ku-band satellite beacon," *Int. J. Phys. Sci.*, vol. 6 no. 7, pp. 1673–1676, Apr. 2011.
[8] N. B. A. Rahim, R. Islam, J. S. Mandeep, H. Dao, and S. O. Bashir, "Tropospheric scintillation prediction models for a high elevation angle based on measured data from a tropical region," *J. Atmospheric Sol.-Terr. Phys.*, vol. 105–106, pp. 91–996, 2003.